Volcanic Jets to Commercial Jets: Synopsis and Diagnosis

Erkan Aydar, H Evren Çubukçu, Çağatay Bal, Nicolas Cluzel, Çağdas Hakan Aladağ, Orkun Ersoy, Didier Laporte

Volcanic Jets to Commercial Jets: Synopsis and Diagnosis

Erkan Aydar[1,3]✉, H. Evren Çubukçu[1], Çağatay Bal[2], Nicolas Cluzel[3], Çağdas Hakan Aladağ[4], Orkun Ersoy[1], Didier Laporte[3]

[1] Hacettepe University, Geological Engineering Department, 06800 Beytepe, Ankara, Turkiye

[2] Muğla Sıtkı Koçman University, Department of Statistics, Muğla Sıtkı Koçman Üniversitesi, 48000 Kötekli/Muğla, Turkiye

[3] Université Clermont Auvergne, CNRS, IRD, OPGC, Laboratoire Magmas et Volcans, F-63000 Clermont-Ferrand, France

[4] Hacettepe University, Department of Statistic, 06800 Beytepe, Ankara, Turkiye

✉Corresponding Author: Erkan AYDAR, eaydar@hacettepe.edu.tr ; now on sabbatical at UCA-LMV

Orcid No Erkan AYDAR: 0000-0002-6550-0714

Abstract

Aircraft encounters with volcanic ash have caused significant damage over the past 40 years, resulting in particular attention being given to the issue. We analyzed the Volcanic Ash-Aircraft Encounter Database published by the USGS. We added new volcanic eruptions and parameters such as eruption types, dry-wet, etc. Then, we applied standard and advanced statistical methods.

Over 130 encounters have been documented in the mentioned database, with volcanic ash causing severe abrasions to the windshield, airframe, wings, and engine components. In nine cases, aircraft engines failed. We applied the binary regression analysis and some laboratory melting experiments on volcanic ash. Besides phreatomagmatism, we use the term external water in this work to describe meteoric water that enters volcanic plumes through precipitation or melting ice on ice-capped volcanoes. We demonstrated that engine failure occurs when our regression analyses undergo dry-to-wet conditions. In other words, Statistically, there is a positive correlation between wet ash encounters with aircraft and engine failure incidents. Moreover, experiments conducted at 900°C and under 40 bar pressure showed increased sintering in the dry sample, while melting textures were more prevalent

in hydrated samples. We concluded that despite the various eruptive dynamics of volcanic ash, the introduction of external water into the volcanic plumes, probably causing instantaneous hydration of volcanic ash, is a common factor in engine failure incidents. Thus, we have identified the reasons behind engine failures during encounters between aircraft and volcanic ash and the specific damage that can occur depending on the type of eruption involved.

Keywords: Ash, Aircraft, Dry-Wet Eruption, Abrasion, Melting, Engine Fail

Statements and Declarations

Competing Interests: The authors declare no competing interests or relationships that could influence the work.

Introduction

The era of jet-powered aircraft began in the 1930s and 40s with the invention of the first jet engine for airplanes. Initially, this invention was mainly used in military applications (Boyne, 2020). However, in the 1950s, it began to be used for regular commercial aviation, starting with the first flight of the de Havilland Comet airliner on May 2, 1952, from London to Johannesburg (Budd et al. 2012). Civil aviation and air transport have experienced a significant increase in demand, expanding at least tenfold since 1970, compared to the 3-4 fold growth of the world economy (IATA 2013). Technological and economic progress have made commercial jets more comfortable, secure, and making the world smaller and countries closer. Airlines have continued to increase the number of city-pair routes globally, and in 2018, almost 22,000 city pairs were regularly serviced by airlines (IATA 2019).

The Catalogues of the Global Volcanism Program by the Smithsonian Institute report that over the past 10,000 years, around 1,500 volcanoes have erupted. Out of these, 550 have had eruptions during recorded history and are considered active, and approximately 55 to 60 volcanoes become active each

year. Some of those volcanic eruptions can generate ash clouds that reach high altitudes (Salinas 2004) during their explosive and intense fragmentation of either erupted magmas or host rocks. The resulting volcanic ash comprises free minerals, pulverized rock fragments, and vesiculated or non-vesiculated juvenile magma particles. They can be injected into the atmosphere up to 45 km from the surface (Wilson et al. 1978). Plumes from volcanic eruptions may vary in height depending on the type of eruption but are typically visible on air routes above 9 km for an average 20-25 days per year for the North Pacific region and perhaps even worldwide (Miller and Casadevall 2000). In fact, in volcanic regions, the number of days with volcanic plumes can be frequent, and altitude may vary greatly. Even short-lived volcanic plumes can impact the economy by disrupting air traffic, as demonstrated during the Eyjafjallajökull 2010 eruption (Hirtl et al. 2020). The threat volcanic ash poses to jet-powered aircraft became significantly more apparent following the high-profile ash encounters of 1982 due to safety reasons in the skies above Indonesia. In one particular incident, two aircraft that were en route to Australia via Indonesia were affected by ash that was emitted from the Galunggung volcano, leading to engine failures (Gourgaud et al. 2000). The first aircraft had to descend more than 25,000 ft before the engines could be restarted (Casadevall 1994). In the case of the second aircraft, three out of four engines stopped functioning while passing through the eruptive cloud (Guffanti et al. 2010). This volcanic eruption and the resulting ash-aircraft encounter marked a significant milestone in aviation history. Although not the only incident of its kind, the Galunggung eruption was pioneering in bringing attention to aviation safety within the international community about volcanic eruptions. In December 1989, another jumbo jet encountered volcanic ash from the eruption of Mt. Redoubt in Alaska (Bayhurst et al. 1991). In 1987, the International Civil Aviation Organization (ICAO) established the International Airways Volcano Watch (Lechner et al., 2017). This initiative includes nine Volcanic Ash Advisory Centers (VAACs) whose main task is to act as an interface between volcano observatories, meteorological agencies, and air traffic control centers

(ICAO 2007). Each VAAC monitors volcanic activity and ash clouds in its designated region using reports from volcano observatories and satellite imagery (ICAO 2007).

After Galunggung-1982, the eruption of Eyjafjallajökull in 2010 brought even more attention to the issue of volcanic ash-aircraft encounters. Clarkson et al (2016), after the Eyjafjallajökull-2010 eruption, re-examined the Galunggung 1982 and Redoubt 1989 incidents from past encounters and stated that engine problems occurred if the ash concentration was 200 mg/m3 and above and 'and that there was negligible damage for relatively short durations of exposure at concentrations below this value..

Volcanic ash is formed due to the fragmentation of magma and/or rock (Zimanowski et al. 2003). This intensive fragmentation makes volcanic ash an angular abrasive material. The abrasiveness of volcanic ash is influenced by its hardness, shape, and density, as well as the impact pressure and velocity exerted on a surface (Stachowiak 2000; Blake et al. 2017). Due to its ability to damage various aircraft parts, such as the airframe, wings, windows, windshields, and engine components, the encounters have a significant impact on flight safety and maintenance costs (Chen and Zhao 2015).

A previous study by Guffanti et al. (2010) provided a comprehensive compilation of incidents involving aircraft encounters with volcanic ash clouds. The study covered the period between 1953 and 2009 and documented 129 incidents, 79 of which resulted in varying degrees of damage to the airframe and/or engines with 9 incidents with engine failure. Moreover, there have been around 113 incidents of aircraft-ash encounters since 2010, according to Christmann et al. (2015) and (2017). These encounters were mostly classified as severity index 2 or lower. Although the authors gave 6 encounters as Severity Class-3, they used only one engine damage incident in detail in their publications (ID: 2010-82). According to this compilation, out of 113, 92 are related to Eyjafjallajökull-2010 and 17 to Grimsvötn-2011, and they actually stand as two statistically weighted

volcanoes in the database. Clarkson and Simpson (2017) have pointed out that the two databases only record exposure events and their outcomes and, however, lack information on all parameters that impact the damage caused by ash. They also add that the two most critical parameters that affect damage are the ash concentration and the duration of time the aircraft and its engines are exposed to the ash cloud (Clarkson and Simpson 2017).

In this paper, however, since there were 103 incidents in two separate eruptions of only two volcanoes, those data were not used to avoid creating an unbalanced distribution in the entire data set. Therefore, we have supplemented and modified the dataset of Guffanti et al (2010) by adding data on several recent eruptions (e.g.Eyjafjallajökull), including information on the types and states of eruptions encountered. As per the report, there have been nine incidents where encounters with ash caused engine failure and shutdown during flights.

In this paper, we first provide an overview of the damage caused by volcanic eruptions and ash encounters, by way of statistical methods...

Secondly, in our statistical study, since we saw that surface water (phreatic, phreatomagmatic, rain, seawater, molten ice, etc.) was involved in the eruption plumes, especially in 9 engine failure incidents, we conducted dry and wet ash melting experiments to observe softening and melting behavior.

METHODS

Statistical Method

The data on volcanic ash-aircraft encounters used in this study is obtained from a USGS report by Guffanti et al (2010). The report is easily accessible and includes a detailed appendix that provides a comprehensive overview of volcanic ash-aircraft encounters from 1953 to 2009. The catalogue is compiled using aircrew statements, published scientific articles, reports (Smithsonian Institution's, NASA), and written and oral explanations. In addition to technical data such as delta distance and height, the catalogue also assesses volcanic eruptions based on their severity index. It is a valuable

resource for researchers and others interested in this topic. We have enhanced the database by incorporating eruption types, the dry-wet state of the eruption, external factorsand other statistical variables. In order to analyze a database that deals with binary classification problems, we employed the method of Binary Logistic Regression. Our goal was to determine the effects and explanation levels of the variables available- explosion, type, and area (independent variables)- on Damage1 (dependent variable), which encompasses the damage caused up to that which led to engine failure. We used regression analysis in SPSS to show the effect of a 1-unit change in the independent variable on the dependent variable. The study excluded observations of missing independent variables, resulting in a total of 99 rows for analysis. In addition to the independent variables, new variables (interactions) were created to measure their effects. The backwards elimination method developed a meaningful model that included these variables. The details of the statistical study are given in supplementary information.

Melting Experiments

To better understand how water affects volcanic ash melting incidents, we conducted melting experiments using a sample from the Nescher PDC flow of Massif Central, France. To start the experiment, we first dried the Neschers PDC ashes in an oven at 80°C for 24 hours. We then discarded the larger grains by sieving under 325 microns. Next, we loaded about 38 mg of the resulting powder into gold capsules, with dimensions of 20 mm in length, 3 and 4 mm outer diameter, and wall thicknesses of 0.2 mm for dry and wet experiments, respectively. We conducted two types of tests on the capsules: dry (on two samples) and with the addition of 1.68 wt% water (on one sample). In our initial experiments, when we added more than 2 wt% of water, the capsules couldn't withstand the internal pressure and burst. Therefore, we decided to reduce the amount of added water to 1.68 wt%, and we also increased the capsule size to avoid any mishaps. The experiments were carried out in a pressure vessel heated externally and mounted on a nitrogen pressure line. The vessel has a maximum

operating pressure of about 300 MPa. The temperature ranges from 800-850°C at high pressure to 900-950°C at low pressure (≤ 100 MPa). Additionally, the autoclave is fitted with a rapid quench extension and an automatic decompression system (Mourtada-Bonnefoi and Laporte 2004; Cluzel et al. 2008). To mimic the natural conditions during ash ingestion by aircraft engines, faster heating is necessary. To achieve this, we have selected a procedure that quickly exposes the sample to the experimental conditions of 900°C and 40 bar. Following the welding process, the capsules were loaded into the pressure vessel at the cooling circuit's level (cold spot). The vessel was then pressurized up to 40 bar and heated to 900°C. Once the temperature reached 900°C, the capsules were rapidly positioned (within a few seconds) at the hot spot of the pressure vessel by lifting the sample holder using an external electromagnet. The experiment was then quenched by lowering the capsules to the cold spot after 30 minutes at 900°C-40 bar. Finally, the samples were studied under SEM and FIB-SEM.

Results: Synopsis on the engine failing eruptions

Mt Galunggung 1982-83 eruption

It was an exceptionally long-lasting eruption of about nine months between April 5 1982-January 8 1983 (Gourgaud et al. 1989). Throughout this eruption, the composition of the erupted magma evolved from andesite (58% SiO2) to Mg-rich basalt (47% SiO2), while the eruption style underwent significant changes over time (Katili and Sudradjat 1984; Sudradjat and Tilling 1984; Gourgaud et al. 1989). Simultaneously with chemical variation and water consumption, the eruption dynamics also changed and occurred in three distinct eruption phases with different eruptive styles. An initial Vulcanian phase (5 April-13 May), a phreatomagmatic phase (17 May-28 October), and a Strombolian phase (3 November-8 January) have been recognised (Katili and Sudradjat 1984; Ersoy et al. 2007). The transition from the Vulcanian to the phreatomagmatic phase resulted in increased eruption explosivity, characterised by higher plume heights (from 5-10 km to 4-20 km), more

extensive deposits, and changes in crater morphology (Gourgaud et al. 2000). Four aircraft encountered volcanic ashes during this eruption. In two of the four encounters, the engines were failed Incident ID: 1982-03 and 1982-06, Guffanti et al 2010). The first engine failed incident occurred on June 24, 1982, at an altitude of approximately 11,2 km (Guffanti et al. 2010). This coincided with the phreatomagmatic eruption phase, with the eruption plume reaching 12-14 km (Katili and Sudradjat 1984). The second incident occurred on July 13, 1982, when the eruption plume reached up to 10-16 km (Casadevall 1994a), and the encounter happened around 10,1 km altitude (Guffanti et al. 2010). This incident also coincided with the phreatomagmatic phase and corresponded to the formation of the second maar crater. In both incidents, after the aircraft had lost significant altitude, the pilots managed to restart the engines and landed (Miller and Casadeval 2000).

Mt St. Helens 25.05.1980 Eruption

On May 25, 1980, at 2:30 a.m., precisely one week after the massive eruption on May 18, Mount St. Helens underwent another eruption phase, marked by the release of dacitic ash. This eruption column reached up to 14 km and was characterized by a Plinian eruption (Lipman and Mullineaux 1980; Harris 1988; Fisher et al. 1998). Before the eruption, there was a sudden surge in earthquake activity while it was raining (Blong 1984; Harris 1988). At that time, an aircraft (L-100/C-130) flew through the clouds filled with ash at an altitude of around 4.5-5 kilometers (Incident ID: 1980-03; Guffanti et al. 2010). Two out of four engines experienced a severe compressor stall, leading the crew to shut them down, and the aircraft had to rely on engines 1 and 3 for the landing (Guffanti et al. 2010).. During subsequent inspections, molten volcanic ash was found in the turbine and abrasion was also found on parts of the engine. Furthermore, the windshield was damaged by abrasion and icing, and the wings showed signs of sandblast damage (Guffanti et al. 2010).

Mt Redoubt December 1989–June 1990 Eruption

The ice-covered Redoubt Volcano in Alaska erupted suddenly, causing the melting of ice and snow resulting in mudflows (Miller and Chouet 1994). The eruption commenced primarily with phreatomagmatic vent-clearing explosions on December 14, 1989, following a seismic crisis (Brantley 1990; Miller and Chouet 1994; Miller et al. 1998). The following day, at least four eruptions rich in ash occurred, with the fourth eruption happening at 10:15 a.m. (Alaskan Standard Time), projecting ash up to 12 km (Miller et al. 1994). The incident occurred at 11:46 a.m. when a Boeing 747-400 travelling from Amsterdam was flying at an altitude of approximately 7000 meters (approx 25000 feet) and encountered Mt Redoubt's ash cloud (Incident ID: 1989-05; Guffanti et al 2010). As a result, all four engines lost power, but the crew restarted them. The plane descended to a height of 4,000 meters (13,000 feet) and landed safely in Anchorage. (Przedpelski and Casadevall, 1991; Casadevall 1994b; Miller et al. 1998).

Mt Pinatubo June 1991 Eruption

During the pre-climactic eruptions of the Pinatubo 1991, there were at least four phreatomagmatic eruptions, particularly on June 14-15, before the onset of the climactic eruption on June 15 (Hoblitt et al. 1996). The dacitic climactic eruption of Pinatubo commenced with the injection of an ash cloud into the stratosphere, reaching heights of 37-42 km (Rossi et al. 2019). This ash cloud circled the globe within 22 days (Casadevall et al. 1996). The height of the ash cloud was significantly higher than typical aircraft cruising altitudes, which generally range between 30,000 and 40,000 feet. Simultaneously with the volcanic eruption, the Philippines was also affected by Typhoon Yunya, and the falling ash was wet (Oswalt et al. 1996). Volcanic ash plumes bursted through the clouds of Typhoon Yunya (Tupper et al. 2005), and all drifted toward SW, affecting some of the world's busiest air traffic corridors (Casadevall et al. 1996). Besides, Guo et al (2004) proposed that ice particles in the Pinatubo cloud form from evaporated and sublimated water transported by Typhoon Yunya, producing significant ice in addition to volcanic ash. Sixteen damaging encounters between aircraft

and ash clouds have been confirmed. Among these encounters, two aircraft experienced engine failures (Incident ID: 1991-17 and 1991-18, Guffanti et al 2010), leading to ten other damaged engines requiring replacement (Casadevall et al. 1996).

Mt Unzen June 1991 Eruption

In June 1991, the volcano produced intense pyroclastic density currents (PDCs), particularly during the eruption on June 3, resulting in the tragic loss of 43 lives, including three volcanologists (Maurice and Katia Krafts, Harry Glicken), who were caught under the block and ash flow (Yamamoto et al. 1993). Although there is no clear information in the literature regarding the height of the eruption column, it is reported that the ash fallout extended up to 250 km away (GVP 1991). The weather conditions during this period were generally rainy, forming ash clusters, accretionary lapilli, and sporadic mudflows caused by the rain (Watanabe et al. 1999). The eruption, which involved the emplacement of domes and associated pyroclastic flows with co-eruptive ashfall, continued until July 1991, occurring amidst rainy weather (Watanabe et al. 1999). According to the Japan Meteorological Agency (JMA), this region receives the highest precipitation in June and July (JMA Website). On June 27, a volcanic ash-aircraft encounter occurred, during which two out of three engines of a DC-10 aircraft stalled at an altitude of approximately 37,000 feet, and the engines were successfully restarted after descending to a lower altitude (Incident ID : 1991-21, Guffanti et al. 2010).

Mt Chaiten 2008 Eruption

The volcanic tremors intensified around Chaitén volcano on May 2, 2008, leading to an initial Plinian-style eruption column that reached a height of 21 km and persisted for 6 hours (Lara 2009). Then, the column heights decreased to 11-16 km during subsequent injections the following day (Folch et al. 2008) until the lava dome was emplaced several days later (Lara 2009). The eruption, which involved the discharge of 4 km3 of crystal-poor rhyolitic magma, produced very fine volcanic ash particles (<4 microns), accounting for approximately 12% of the total emitted volume (Carn et al. 2009). Due to

Chaitén's location in a region with high annual precipitation of 2400 mm, the eruption clouds from the volcano inevitably interacted with the humid atmosphere (Forte 2018). Meanwhile, the weather was rainy during the initial phases of the eruption (the first week of) May 2008 (Pierson et al.2013). Five ash-aircraft encounters were reported with engine troubles or the presence of unmelted ash in the engines (Incident ID: 2008-01, 2008-02, 2008-03; Guffanti et al. 2010). Notably, one aircraft encountered the ash cloud at low altitudes during landing but could not take off from Bariloche airport in Argentina, located approximately 225 km from the volcano, due to a lack of engine power (Guffanti et al. 2010).

Mt Soufriere Hills, July 2001 Eruption

The Soufriere Hills volcano in Montserrat, which became active for the first time in recorded history in 1995, has since experienced periodic growth of andesitic domes, accompanied by pyroclastic flows and Vulcanian eruptions (Young et al. 1997; Druitt et al. 2002; Herd et al. 2005). The volcano has remained active since 1995. On July 27, 2001, a volcanic ash-aircraft encounter occurred during an andesitic dome emplacement, resulting in a block and ash flow forming an eruption cloud rising to 11 km (Wadge et al. 2014). The dome collapse coincided with the heavy rainfall (Matthews et al. 2002; Wadge et al. 2014). In addition, an ash-aircraft encounter at 24000 feet has been reported with engine shutdown in flight (Incident ID: 2001-02, Guffanti et al. 2010) with numerous other encounters resulting in abrasion damage (Guffanti et al. 2010).

Mt Manam July 2006 Eruption

Manam is an active volcano in Papua New Guinea, known for emitting generally basaltic materials with Strombolian-style eruptions (Tupper et al. 2007a). While the eruption column usually remains low, reaching only a few kilometers in height, there are instances when volcanic products can be propelled over 10 km with subplinian columns (Tupper et al. 2007a). On July 17, 2006, a survey

aircraft experienced engine flame-out at a high altitude of approximately 11.9 km over Papua New Guinea, near the vicinity of Manam volcano (Tupper et al. 2007b). Fortunately, the engines were successfully restarted at lower altitudes (Tupper et al. 2007b).

In spite of the clear weather and lack of sulfur odor, the plane experienced engine failure while flying over Papua New Guinea near Manam Volcano (Incident ID: 2006-03, Guffanti et al. 2010). The investigations revealed that a part of the fuel system were clogged by the ash (Tupper et al. 2007b). It is also suggested that ice-coated ash would have caused the failure (Tupper et al. 2007b).

Mt Eyjafjallajökull April 2010 Eruption

The eruption of Mt. Eyjafjallajökull in April 2010 began with the emission of basaltic lava as a flank eruption on March 20. It was followed by trachyandesite eruptions from the summit on April 14-16, which had a significant impact on European air traffic (Sigmundsson et al. 2011). The volcanic activity originated from the caldera on the summit, beneath 200-300 meters of ice, resulting in mudflows and the release of very fine-grained volcanic ash that reached a height of 10 km (Gislason et al. 2011). The eruption continued for 39 days throughout April and May, with ash reaching heights of 3-10 km due to various explosive events (Gudmundsson et al. 2012). Christmann et al (2015) state that there were 92 volcanic ash-aircraft encounters in the Eyjafjallajökull 2010 eruption and that the severity class in these encounters was generally 0 and 1 and subordinate severity class 2 with less abrasion and physical damage. In addition, Christmann et al. (2015) stated that in Incident ID: 2010-82, a two-engine aircraft was exposed to the smell of sulfur at 6000 ft and that there were fluctuations in engine pressure when it landed, and this situation did not improve and classified this incident as Severity class 3.

Results: Diagnosis

In volcanic ash-aircraft encounters, little attention has been paid to the type of volcanic eruption, magma chemistry, and external factors influencing the eruption. Instead, the focus is on the type,

severity and rate of damage caused to the aircraft and the "Severity Index for aircraft encounters with volcanic ash clouds" was established (ICAO 2007). The objective of our study is to relate the encounters and the damage they caused with eruption types and external factors. We analyzed the current situation using a modified database (compiled initially by Guffanti et al. 2010) and applied standard and advanced statistical methods to achieve this. Additionally, we sought to validate our findings by conducting ash-melting experiments.

Statistical analysis

The synthesis we made regarding the volcanic eruptions in the database we used is presented in SI-Table. 1. In addition to the phreatomagmatism due to the interaction of magma-surface water, we mean, by the external water, meteoric water introduced into the volcanic plume due to melting of ice-clad on volcanoes, rainy conditions, rainstorms, typhoons, air moisture causing the ice particles, etc. In our comparative evaluations of aircraft encounters with volcanic ash, the introduction of external water during the volcanic eruption phase, in the eruption cloud or the eruptive products, is a key parameter that determines the consequences of the encounter. Accordingly, we regrouped the eruptions in the database (SI-Table 1) under the headings of Plinian-Dry (without external water), Plinian-Wet (with external water), Subplinian-Strombolian, Pelean, Vulcanian-Dry, Vulcanian-Wet and Phreatomagmatic. Note that our nomenclature of Dry vs. Wet refers only to external water: the magmas at the origin of the explosive eruptions studied have high initial water contents (several wt%), but almost all of this magmatic water is lost by degassing during magma ascent and eruption.

The statistical distribution of damage due to aircraft encounters with volcanic ash is shown as a function of volcanic eruption types in Fig.1 (SI-Table 2). Accordingly, Plinian-Dry and Vulcanian-Dry eruptions are the ones that have most affected the aircrafts. Plinian-Dry material can cause abrasion in both the airframe (including windows, windshield, and all flight components, etc.), the engine, and some subordinate amount of blockages in the engine parts.

On the other hand, Vulcanian-Dry material only abrades the airframe and flight components. Some Strombolian-Subplinian eruptions created a volcanic cloud up to the aircraft's flight altitude. In general, their products cause damage in sandblasting, cracking and abrasion or scratch on windshields, on leading edges of wings, on aircraft fuselage, and sometimes in engine blades.

Pelean eruptions are mainly characterized by the growth and collapse of lava domes and the formation of pyroclastic flows. In the database of ash-aircraft encounters, there are only a few instances of Pelean eruptions, but the abrasive effect is still noticeable. We did not differentiate between dry and wet cases for the Pelean type, as there were only a few incidents. However, it is important to remember the impact of rain during the Soufriere Hills-Montserrat eruptions in 2001 and the Unzen eruptions in 1991. We want to emphasize that engine failures were only observed during eruptions when external water was present. Such eruptions include Plinian-Wet, Pelean eruptions during rainy conditions (examples: Soufriere Hills and Unzen), Phreatomagmatic eruptions, and Vulcanian-Wet eruptions. Additionally, it should be noted that ice-coated basaltic ash, as shown in the 2006 Manam eruption (Tupper et al. 2007b), should also be added to this list. Moreover, we performed statistical regression analysis to evaluate together variables that affected the eruptions and caused damage to aircraft. The detailed analysis and the results are given in SI-Statistic. We defined the following variables: Area (values: Tropic, Subtropic, etc.), Type (values: Wet, Dry), Explosion (values: Strombolian – 1, Vulcanian-Dry – 2, Pelean – 3, Plinian-Dry – 4, Plinian-Wet – 5, Vulcanian-Wet – 6, Phreatomagmatic – 7, with the explosivity increasing from value 1 to 7), Damage 1 (values: Engine fail, other), and Damage 2 (values: Engine fail, Engine problem, Windshield problem, Other damage, No damage). Applied Binary Logistic Regression uses regression analysis to determine the effects and explanation levels of the independent variables on Damage 1 (the dependent variable), which indicates the damage status of the aircraft. Regression analysis measures the effect of a one-unit change in the independent variable on the dependent variable. The variables related to the model, in

which the contribution of each independent variable in the model is significant, are the variables that include the combined effect of the explosion, type, and explosion-type variables.

The effect of the Explosion variable on the Damage 1 variable is statistically significant but with the lowest score: Damage 1 varies by approximately 1.3 unit in the negative direction for a one-unit change of Explosion. In other words, as the explosion type increases, the engine fail state emerges. Besides, the relationship between variables Type (Wet vs. Dry) and Damage 1 is statistically significant, with an effect of approximately 5.2 units on Damage 1 in the negative direction. In other words, as the introduction of external water increases, the probability that the engine fails also increases statistically significantly. Moreover, the independent variable formed by the variables Explosion and Type taken together (interaction) positively affects the variable Damage 1 and has an odds ratio of 2.4. Therefore, if the Explosion and Type variables increase by 1 unit, the Damage 1 variable is 2.4 times more likely to appear with the " other " value.

Besides, after getting significant results of logistic regression with binary response variable `Damage1` with categories `Engine fail` and `Others`, it is found that the `type` variable, which indicates dryness-wetness, has the most potent effect on the engine fail. The odds of the occurrence of the `Engine fail` rising by wetness can also be seen in Fig2. Additionally, a more in-depth analysis was intended by investigating the response variable `Damage 2` by categorizing it into five classes as: `Engine fail`, `Engine Problem`, `Windshield problem`, `Other damage` and `No damage`. Regrettably, due to insufficient data, the observed data points were not distributed uniformly into five categories, rendering the results insignificant. However, individual categories such as `Engine problem` and `Windshield problem` with substantial data points have shown promising results compared to the reference category `No Damage`.

To put it simply, the transition from a "dry" state to a "wet" state has a statistically significant correlation with the occurrence of "Engine Fail".

Melting Experiments

To understand the relationship between the introduction of external water and the damage due to volcanic ash-aircraft encounters, we performed experiments to test the effect of water on volcanic ash melting. Ashes from Neschers pyroclastic density current (PDC), Monts Dore stratovolcano, French Massif Central, were used as starting material. It has a trachytic composition (63.0 wt% SiO_2 and 10,8 wt% $Na_2O + K_2O$ on a volatile-free basis). It is principally composed of green clinopyroxene and feldspars, fragments of pumice, glass shards and xenoliths (Fig3). It is dated at 0.58 ± 0.02Ma (39Ar/40Ar; Lo Bello et al. 1987).

SEM images of the starting material reveal that the pumices are tubular, generally unaltered and appear very clean (Fig3). Glass shards also do not exhibit alteration but show minute particles adhering to their surfaces. Some glass shards also display vesiculated textures. Apart from adhering particles, no basic alteration was observed on feldspars or clinopyroxenes. All fragments are angular, and no evidence of melting was observed on the components (Fig3 and SI-Fig1).

Neschers volcanic ash was loaded in gold capsules, either dry or along with 1.7 wt% water, and subjected to a temperature of 900 °C and a pressure of 40 bar for half an hour in an externally heated pressure vessel specifically modified to closely reproduce the natural conditions during ash ingestion by aircraft engines. At the end of the experiment, both the anhydrous (NAsh-AnH) and hydrous samples (NAsh-H) display very different textural features in comparison to the starting material (Fig4, SI-Fig2 and SI-Fig3). The samples have become coherent compared to their initial ashy state. The specimens comprise mainly alkaline mineraloids (mineral gel), prismatic minerals, acicular minerals, relict minerals, and relict pumices components (Fig5; SI-Fig3). First, the volcanic ash powder has become more cohesive due to the effect of sintering, and the starting grains are welded together. Moreover, in addition to relics of the original minerals and fragments that commonly show traces of incipient melting, we observe ubiquitous surface encrustation by newly grown acicular or prismatic crystals (Fig5; SI-Fig3).

Description of the anhydrous sample

It is dominated by microspheres with diameters of up to 50 microns but generally between 10-20 microns. The background consists of rounded, spherical, ellipsoidal, bulbous, and globular material, and their surface is extremely ragged; overall, they constitute a botryoidal cluster (Fig.4A-B). Moreover, the matrix bears some droplets (Fig. 6A).

Some tubular pumice fragments and most prismatic minerals are still conserved, although some pumice exhibits incipient melting starting from the rim (Fig.6.B). Newly grown acicular, prismatic, and tabular crystals with grain sizes smaller than 10 microns are ubiquitous in the sample, adhering to the pumice fragments, the glass shards and the larger minerals. The fibrous, acicular crystals are in bundles and sometimes grow outward from the prismatic minerals.

Description of the hydrous sample

The textural properties of the hydrous sample are quite similar to those of the anhydrous sample, except that the evidence of melting is more systematically developed in the former than in the latter. Melting is visible on the edges of the pumice fragments, on the glass shards and mineral surfaces, and is responsible for forming microspheres, droplets, and other rounded shapes (Fig.4C &Fig. 6C-D). Moreover, in the encrustations which cover the surface of the original grains, the small euhedral crystals rest on a glassy material in which they are more or less immersed (Fig. 5). In particular, laser engraving of the wet sample exhibits rounded, stepped structures. In contrast, the anhydrous sample shows a much more homogeneous internal structure (Fig.7). In particular, the bulgeous chaotic surface and step-like glassy texture are more evident in the melting progression (Fig.7). The surface dissolution and acicular minerals are ubiquitous in the wet sample (Fig.7). Similar aspects were not found in the anhydrous sample engraving (Fig.7).

Finally, our experiments show that adding water increases the degree of fusion and, therefore, the "stickiness" of the volcanic ash and its ability to adhere to the walls of the jet engine turbines.

Discussion

Volcanological information is crucial to understand better the damage caused by ash in volcanic ash-aircraft encounters (Davison and Rutke 2014). Plinian-type eruptions significantly impact aviation operations due to their wide regional dispersion, while Vulcanian and Surtseyan-type (Phreatomagmatic) explosions are more circumvented and can be avoided (Davison and Rutke 2014). Although Plinian eruptions can have a global impact, with eruption clouds reaching heights of 45 km (Wilson et al. 1978), the eruption of Eyjafjallajökull in 2010 had a worldwide effect despite the plume not exceeding 10 km. (Gudmundsson et al. 2012). Magma supply rate, sustainable eruption conditions, and wind directions influence this variation.

Volcanic ash is highly variable in both chemical composition and physical characteristics, and its particle morphology can change during an eruption (Cioni et al. 2014). It is natural to anticipate that the abrasiveness of volcanic ash will differ based on various factors, such as the dynamics of eruption/fragmentation, chemical composition, viscosity, volatile contents, ejection rates, and internal and external factors. This means that the abrasiveness can vary significantly between eruptions or even within a single eruption. However, despite its importance, this question remains poorly understood at present. The main damage caused by volcanic ash is the wear effect of ash on the aircraft airframe, windshields, electronic parts and engine fuel systems.

Statistically, Plinian-type eruptions cause the most damage to the aircraft body and engine (Fig.1). Besides, Vulcanian-dry eruptions also have a significant impact on sandblasting, particularly affecting the windshield, wings and airframe. According to the damage-eruption type diagram (Fig1), volcanic ashes of dry eruptions cause damage mostly through physical effects. These are generally damage such as abrasion, cracking, sandblasting, and engine problems.

Our regression analysis shows a meaningful correlation between engine failure incidents and external water contributions to eruptive sequences. It reveals a significant increase in engine failure rates during the transition from dry to wet conditions. Consequently, Plinian-wet eruptions stand out as the type of volcanic activity that causes the most engine failures. Besides, the engine failure incident related to the Pelean style eruption in Fig1 is related to the Soufriere Hills and Unzen eruptions, where heavy rain conditions have been reported. This article shows that external water is involved in an eruptive sequence in engine fail incidents with molten glass inside the engine. However, of course, these meltdowns cause technical malfunctions in the engines. Is it possible that this is a coincidence? Numerous studies have focused on ash melting, particularly following the Eyjafjallajökull eruption in 2010 (Kueppers et al. 2014; Song et al. 2016; Song et al. 2017; Giehl et al. 2017; Müller et al. 2020; Pearson and Brooker 2020). The softening temperatures of glassy volcanic ash can be as low as 600°C, and complete sintering occurs at temperatures as low as 1050°C (Kueppers et al. 2014). Jet engines' high temperatures (1200-2000°C) worsen the impact of volcanic ash by melting and sticking to turbine parts (Song et al. 2016). While most melting experiments involved heating specimens from room temperature in an autoclave, gradually reaching the melting point, our study employed a faster heating technique in which the cold ash (at room temperature) was rapidly exposed to a hot environment of 900°C under 40 bar pressure, mimicking the conditions proposed for a Rolls Royce turbofan engine (Giehl et al. 2017). In real-life scenarios, it would be more practical to expedite the melting process by freezing the ash material at an air temperature consistent with the flight altitude. This should be done before subjecting it to the autoclave. This is because the tops of Plinian eruption clouds are exposed to extremely cold temperatures, reaching as low as -50°C (Williams and McNutt 2004) or -88°C during the Pinatubo 1991 eruption (Lynch and Stephens 1996).

In recent years, studies have begun to be carried out on the rehydration of volcanic ashes during subaerial, submarine eruptions with external water contributions (Hudak et al 2021; Hudak et al 2022; Mitchell et al 2021). It is known that the rehydration of volcanic glass develops over time, starting

from atmospheric water as post-eruptive/post-depositional (Seligman et al 2016). Besides, volcanic glasses hydrate faster if they encounter water under high-temperature conditions during the eruption, transport and deposition (Hudak et al 2022). Song et al (2016) simulated the behavior of volcanic ash when ingested in jet engines. They tested different heating rates ranging from 10 to 40ºC per minute and observed that water was mostly released during heating at temperatures between 600-700ºC. Tg (glass transition temperature) is significantly affected by the water content in the material upon heating, as the water content increases, Tg tends to decrease (Giordano et al 2005). Moreover, Hudak et al. (2021) proposed, based on their hydrogen isotope analysis of the volcanic ashes of the Redoubt 2009 eruption, that syn-eruptive hydration occurred in the margins of the eruptive column/plume where glacial meltwater entrained. In this study, we classified eruptions as either dry or wet. Our definition of a dry eruption is relative, as explosive magmas can naturally contain around 6-7% water (Williams and McNutt 2004). On the other hand, wet eruptions refer to cases where external water contributes to volcanic activity.

In the classical petrological definition, when water or other volatiles are added to the solid during magma generation processes, the melting temperature decreases, and the amount of the melts increases. This type of melting, known as flux melting, was also tested in our experiment, and we observed its contribution to sintering and melting. Our starting material was also trachyte with approximately 10% alkaline content, facilitating flux melting. While the textural properties of dry and wet samples are similar, melting textures are more prevalent in wet samples. It should also be emphasized that the minerals formed after melting are due to the low-temperature crystallization from the mineral gel.

The source of external water within the volcanic plume may be related to phreatomagmatism, atmospheric moisture, or environmental water over which pyroclastic density currents (PDCs) flow and seawater (Joshi and Jones 2009). Any convective cloud, especially in the humid tropics, will consequently drag in moist air whether it rains or not. In this case, atmospheric water can also be

considered regardless of physical state (gas, liquid, solid), as an external water source. Besides the syn-eruptive water involvement, the high relative air humidity in tropical areas may form ice particles. The jet engines can ingest atmospheric ice during flights, and more than 150 related damage have been reported (Haggerty et al. 2019). The presence of ice particles, including ice-coated ash particles in volcanic plumes, is also recognized (Rose et al. 1995; Prata and Rose 2015). While atmospheric ice is a threat to aviation on its own, ice-coated ash grains pose a significant hazard (Prata and Rose 2015). The incident involving an aircraft following the Manam Strombolian-Subplinian eruption is proposed to be related to this phenomenon (Tupper et al. 2007b). Furthermore, external water input to volcanic clouds can occur through heavy rain during the eruption. The Yunya Typhoon, for example, significantly affected the region during the Pinatubo eruption in 1991, contributing a substantial amount of water to the eruption cloud and facilitating the formation of sufficient ice (Guo et al. 2004). Similar heavy rainfall during the Soufriere Hill, Unzen, and Chaiten eruptions also led to the incorporation of water into volcanic clouds.

In addition, apart from water coming into aircraft engines from outside, burning kerosene in the combustor produces a substantial amount of H2O, around an order of magnitude more than is likely to be ingested into the engine inlet from atmospheric water or ice (Rory Clarkson pers comm). The influence of the H2O produced from burning kerosene than when engines ingest water with volcanic ash needs further research as part of future work.

Conclusion

1-We statistically examined the distribution of damage types in Volcanic ash-aircraft encounters according to volcanic eruption types.

2- We defined eruptions as wet when external water is included in the eruptive sequence, plume or column. Others were defined as dry eruptions.

3- The dry eruptive plumes primarily cause abrasion on aircraft. In contrast, our binary regression analysis shows that wet clouds and melting of volcanic ash in the jet engine are positively correlated with engine failure events during these encounters.

4- When we carried out the dry and wet melting experiments by dropping the samples directly into the pressurized hot environment under 900°C and 40 bar pressure to achieve faster heating. Faster heating and water availability facilitate the softening and adhesion of the volcanic ash to hot engine parts. We observed that sintering started in the dry and wet samples, and even melting started, and droplets and spheres were formed, especially in wet conditions. This information may help aviation experts make informed decisions to ensure aircraft safety during volcanic eruptions.

5- While our study is not conclusive, we hope it will encourage further scientific and engineering investigations into the effects of hydrous volcanic ash on aircraft, particularly its various species.

References

Bayhurst GK, Wohletz KH, Mason AS (1991) A Method for Characterizing Volcanic Ash from the December 15, 1989, Eruption of Redoubt Volcano, Alaska. Proceedings of First International Symposium on Volcanic Ash and Aviation Safety. 13-17.

Blake DM, Wilson TM, Cole JW, Deligne NI, Lindsay JM (2017) Impact of Volcanic Ash on Road and Airfield Surface Skid Resistance. Sustainability, 9, 1389.

Blong RJ (1984) Volcanic Hazards: A Sourcebook on the Effects of Eruptions: Academic Press, Sydney, 424 p

Boyne WJ (2020) The jet age in History of Flights in Crouch, T.D., Bilstein, R.E., Boyne, W.J., and others. Encylopedia Britannica, 2020. (https://www.britannica.com/technology/history-of-flight)

Brantley SR (1990) The Eruption of Redoubt Volcano, Alaska, December 14, 1989-August 3 l, 1990. U.S. Geol. Surv., Circ. 1061, 33 pp

Budd LCS, Bell M, Warren AP (2012) Taking Care in the Air: Jet Air Travel and Passenger Health, a Study of British Overseas Airways Corporation (1940–1974). Social History of Medicine, 25/2, 446–461. Doi: 10.1093/shm/hkr115

Carn A, Pallister JS, Lara L, Ewert JW, Watt S, Prata AJ, Thomas RJ, Villarosa G (2009) The Unexpected Awakening of Chaitén Volcano, Chile. EOS, 90, Number 24, 205–212

Casadevall TJ (1994a) Introduction. Proceedings of First International Symposium on Volcanic Ash and Aviation Safety. US Geological Survey Bulletin, 2047, 1-3.

Casadevall TJ (1994b) The 1989-1990 eruption of Redoubt Volcano, Alaska: impacts on aircraft operations. Journal of Volcanology and Geothermal Research. 62, 301-31

Casadevall TJ, Delos Reyes PJ, Schneider DJ (1996) "The 1991 Pinatubo Eruptions and Their Effects on Aircraft Operations," in Fire and Mud: Eruptions and Lahars of Mount Pinatubo, Philippines. Editors C.G. Newhall, and R.S. Punongbayan (Quezon City, PHIVOLCS and Seattle: Univ of Washington Press), 1071–1088.

Chen WR, Zhao LR (2015) Review – Volcanic ash and its influence on aircraft engine components. Asia-Pacific International Symposium on Aerospace Technology, APISAT2014. Procedia Engineering, 99, 795 – 803.

Christmann C, Nunes RR, Schmitt AR, (2015) Recent Encounters of Aircraft with Volcanic Ash Clouds. Deutscher Luft- und Raumfahrtkongress, Document ID: 370124.

Christmann C, Nunes RR, Schmitt AR, Guffanti M (2017) Flying into Volcanic Ash Clouds: An Evaluation of Hazard Potential. NATO Conference: NATO STO AVT-272 Specialists' Meeting on "Impact of Volcanic Ash Clouds on Military Operations" May 2017, Public release, 18p. Doi:10.14339/STO-MP-AVT-272

Cioni R, Pistolesi M, Bertagnini A, Bonadonna C, Hoskuldsson A, Scateni B (2014) Insights into the Dynamics and evolution of the 2010 Eyjafjallajökull summit eruption (Iceland) provided by volcanic ash textures. Earth and Planetary Science Letters, 394, 111–123.

584

585 Clarkson RJ, Majewicz EJE and Mack P (2016) A re-evaluation of the 2010 quantitative
586 understanding of the effects volcanic ash has on gas turbine engines. Proc IMechE Part G. J Aerospace
587 Engineering. 1–18. Doi: 10.1177/0954410015623372
588
589 Clarkson R, Simpson H (2017) Maximising Airspace Use During Volcanic Eruptions: Matching
590 Engine Durability against Ash Cloud Occurrence in: STO-MP-AVT-272, NATO STO, 2017, pp. 1–
591 20.
592
593 Cluzel N, Laporte D, Provost A, Kannewischer I (2008) Kinetics of heterogeneous bubble nucleation
594 in rhyolitic melts: Implications for the number density of bubbles in volcanic conduits and for pumice
595 textures. Contrib. Mineral. Petrol. 156: 745-763.
596 Davison CR, Rutke TA (2014) Assessment and Characterization of Volcanic Ash Threat to Gas
597 Turbine Engine Performance. Journal of Engineering for Gas Turbines and Power. 136 / 081201-1.
598
599 Druitt T, Young S, Baptie B, Bonadonna C, Calder ES, Clarke AB, Cole PD, Harford CL, Herd RA,
600 Luckett R, Ryan G, Voight B (2002) Episodes of cyclic Vulcanian explosive activity with fountain
601 collapse at Soufriere Hills Volcano, Montserrat. In: Druitt, T. & Kokelaar, B. (eds) The Eruption of
602 Soufriere Hills Volcano, Montserrat, from 1995 to 1999. Geological Society, London, Memoirs, 21,
603 281 – 306.
604
605 Ersoy O, Gourgaud A, Aydar E, Chinga G, Thouret JC (2007) Quantitative SEM analysis of volcanic
606 ash surfaces: application to the 1982-83 Galunggung eruption (Indonesia). Geological Society of
607 America. 119 (5-6): 743-752
608
609 Fisher RV, Heiken G, Hulen J (1998) Volcanoes: Crucibles of Change. Princeton University Press.
610 ISBN 978-0-691-00249-1.
611
612 Folch A, Jorba O, Viramonte J (2008) Volcanic ash forecast – application to the May 2008 Chaitén
613 eruption. Nat. Hazards Earth Syst. Sci. 8, 927–940.
614
615 Forte BP (2018) New insights into the characteristics and dynamics of rhyolite long-lasting volcanic
616 eruptions. PhD Thesis. Johannes Gutenberg University Mainz. 193p
617

618 Giehl C, Brooker RA, Marxer H, Nowak M (2017) An experimental simulation of volcanic ash
619 deposition in gas turbines and implications for jet engine safety. Chemical Geology. 461, 160-170.
620 Doi: 10.1016/j.chemgeo.2016.11.024
621
622 Giordano D, Nichols AR, Dingwell DB (2005) Glass transition temperatures of natural hydrous melts
623 : a relationship with shear viscosity and implications for the welding process. J. Volcanol. Geotherm.
624 Res. 142,105–118
625
626 Gislason SR, Hassenkam T, Nedel S, Bovet N, Eiriksdóttir ES, Alfredsson HA, Hem CP, Balogh ZI,
627 Dideriksen K, Oskarsson N, Sigfusson B, Larsen G, Stipp SLS (2011) Characterization of
628 Eyjafjallajökull volcanic ash particles and a protocol for rapid risk assessment. PNAS 108/18, 7307–
629 7312.
630
631 Global Volcanism Program (1991) Report on Unzendake (Japan) (McClelland, L., ed.). Bulletin of
632 the Global Volcanism Network, 16:5. Smithsonian Institution. Doi: 10.5479/si.GVP.BGVN199105-
633 282100
634
635 Gourgaud A, Thouret JC, Bourdier JL (2000) Stratigraphy and textural characteristics of the 1982±83
636 tephra of Galunggung volcano (Indonesia): implications for volcanic hazards. Journal of Volcanology
637 and Geothermal Research 104,169-186.
638
639 Gourgaud A, Camus G, Gerbe MC, Morel JM, Sudradjat A, Vincent PM (1989) 1982 -83 eruption of
640 Galunggung (Indonesia): A case study of volcanic hazards with particular relevance to air navigation,
641 in Latter, J.H., ed., International Association of Volcanology and Chemistry of the Earth's Interior
642 Proceedings in Volcanology 1. Volcanic Hazards: Berlin, Springer, p. 151–162.
643
644 Gudmundsson MT, Thordarson T, Höskuldsson A, Larsen G, Björnsson H, Prata FJ, Oddsson B,
645 Magnusson E, Högnadóttir T, Petersen PN, Hayward CL, Stevenson JA, Jónsdóttir I (2012) Ash
646 generation and distribution from the April-May 2010 eruption of Eyjafjallajökull, Iceland. Scientific
647 Reports 2: 572. Doi: 10.1038/srep00572
648
649

650 Guffanti M, Casadevall TJ, Budding K (2010) Encounters of aircraft with volcanic ash clouds; A
651 compilation of known incidents, 1953–2009: U.S. Geological Survey Data Series 545, ver. 1.0, 12 p.,
652 plus 4 appendixes including the compilation database, available only at http://pubs.usgs.gov/ds/545.
653
654 Guo S, Rose WI, Bluth GJS, Watson IM (2004) Particles in the great Pinatubo volcanic cloud of June
655 1991: The role of ice. Geochem. Geophys. Geosyst. 5, 1-35. Q05003. Doi:10.1029/2003GC000655.
656
657 Haggerty J, Defer E, De Laat A, Bedka K, Moisselin JM, Potts R, Delanoë J, Parol F, Grandin A,
658 Divito S (2019) Detecting Clouds Associated with Jet Engine Ice Crystal Icing. Bulletin of American
659 Meteorological Society, 31-40.
660
661 Harris SL (1988) Fire Mountains of the West: The Cascade and Mono Lake Volcanoes. Mountain
662 Press Pub. Co. Missoula, Montana: 379p.
663
664 Hayward K, (2011) Flying Through an Era of Volcanic Ash. A Discussion Paper by the
665 Royal Aeronautical Society. 1-7.
666
667 Herd RA, Edmonds M, Bass VA (2005) Catastrophic lava dome failure at Soufrière Hills Volcano,
668 Montserrat,12–13 July 2003. J. Volcanol. Geotherm. Res.148, 234–252
669
670 Hirtl M, Arnold D, Baro1 R, Brenot H, Coltelli M, Eschbacher K, Hard-Stremayer H, Lipok F, Maurer
671 C, Meinhard D, Mona L, Mulder MD, Papagiannopoulos N, Pernsteiner M, Plu M, Robertson L,
672 Rokitansky CH, Scherllin-Pirscher B, Sievers K, Sofiev M, Som de Cerff W, Steinheimer M, Stuefer
673 M, Theys N, Uppstu A, Wagenaar S, Winkler R, Wotawa1 G, Zob F, Zopp R (2020) A volcanic-
674 hazard demonstration exercise to assess and mitigate the impacts of volcanic ash clouds on civil and
675 military aviation. Nat. Hazards Earth Syst. Sci. 20, 1719–1739. Doi: 10.5194/nhess-20-1719-2020
676
677 Hoblitt RP, Wolfe EW, Scott WE, Couchman, MR, Pallister JS, Javier D (1996) The Preclimactic
678 Eruptions of Mount Pinatubo, June 1991. In Fire and Mud: Eruptions and Lahars of Mount Pinatubo,
679 Philippines. Editors C.G. Newhall, and R.S. Punongbayan (Quezon City, PHIVOLCS and
680 Seattle: Univ of Washington Press) 457–511.
681

682 Hudak MR, Bindeman IN, Loewen MW, Giachetti, T (2021) Syneruptive hydration of volcanic ash
683 records pyroclast-water interaction in explosive eruptions. Geophys. Res. Lett. 48, 1–8. Doi:
684 10.1029/2021GL094141
685
686 Hudak MR, Bindeman IN, Watkins JM, Lowenstern JB (2022) Hydrogen isotope behavior during
687 rhyolite glass hydration under hydrothermal conditions. Geochimica et Cosmochimica Acta 337, 33-
688 48
689
690 IATA (2013) Annual Review. 60p.
691 (www.iata.org/contentassets/c81222d96c9a4e0bb4ff6ced0126f0bb/iata-annual-review-2013 en.pdf)
692
693 IATA (2019) Annual Review. 30 p.
694 (www.iata.org/contentassets/c81222d96c9a4e0bb4ff6ced0126f0bb/iata-annual-review-2019.pdf)
695
696 ICAO (2007) Manual on Volcanic Ash, Radioactive Material and Toxic Chemical Clouds, 2nd ed.,
697 International Civil Aviation Organization, Montreal, Canada, ICAO Document No. 9691-AN/954.
698
699 Joshi MM, Jones GS (2009) The climatic effects of the direct injection of water vapour into the
700 stratosphere by large volcanic eruptions. Atmos. Chem. Phys. 9, 6109–6118.
701
702 Katili JA, Sudradjat A (1984) Galunggung: The 1982–83 Eruption: Bandung, Volcanological Survey
703 of Indonesia, p. 1–102.
704
705 Kueppers U, Cimarelli C, Hess KU, Taddeucci J, Wadsworth FB, Dingwell DB (2014) The thermal
706 stability of Eyjafjallajökull ash versus türbine ingestion test sands. J. Appl. Volcanol. 3:4.
707
708 Lara LE (2009) The 2008 eruption of the Chaitén volcano, Chile: A preliminary report. Andean
709 Geol. 36(1), 125–129.
710
711 Lechner P, Tupper A, Guffanti M, Loughlin S, Casadevall T (2017) Volcanic Ash and Aviation—
712 The Challenges of Real-Time, Global Communication of a Natural Hazard. In: Fearnley, C.J., Bird,
713 D.K., Haynes, K., McGuire, W.J., Jolly, G. (eds) Observing the Volcano World. Advances in
714 Volcanology. Springer, 51-64. https://doi.org/10.1007/11157_2016_49
715

716 Lipman PW, Mullineaux DR (1981) The 1980 eruptions of Mount St. Helens, Washington: U.S.
717 Geological Survey Professional Paper 1250, 844 p.
718
719 Lo Bello P, Féraud G, Hall CM, York D, Lavina P, Bernat M (1987) 40Ar/39Ar step heating and
720 laser fusion dating of a quaternary pumice from Neschers, Massif Central, France: The defeat of
721 xenocrystic contamination. Chemical Geology 66, 61-71.
722
723 Lynch JS, Stephens G (1996) Mount Pinatubo: A Satellite Perspective of the June 1991 Eruptions, In
724 Newhall,C.G.,Punongbayan,R.S.(Eds.),Fire and Mud:Eruptions and Lahars of Mount Pinatubo,
725 Philippines, pp. 637–645. Philippine Institute of Volcanology and Seismology and University of
726 Washington Press,Quezon City, Seattle and London
727
728 Matthews AJ, Barclay J, Carn S, Thompson G, Alexander J, Herd R, Williams C (2002)
729 Rainfall-induced volcanic activity on Montserrat. Geophysical Research Letters 29(13): 22/1-22/4
730
731 Miller TP, Casadevall TJ (2000) Volcanic Ash Hazards to Aviation: in Encyclopedia of Volcanoes,
732 ed: Sigurdsson H. Academic Press, San Diego, California, USA, p. 915-930.
733
734 Miller P, Chouet BA (1994) The 1989–1990 eruptions of Redoubt volcano: an introduction. Journal
735 of Volcanology and Geothermal Research 62 (1), pp. 1–10
736
737 Miller TP, McGimsey RG, Richter DH, Riehle JR, Nye CJ, Yount ME, Dumoulin JA (1998)
738 Catalogue of the historically active volcanoes of Alaska. U.S. Geological Survey Open-File Report
739 98-0582, 104.
740
741 Mitchell SJ, Hudak MR, Bindeman IN, Carey RJ, McIntosh IM, Houghton BF, Rubin KH (2022)
742 Isotopic signatures of magmatic fluids and seawater within silicic submarine volcanic deposits.
743 Geochim. Cosmochim. Acta 326, 214–233. Doi: 10.1016/j.gca.2022.03.022
744
745 Mourtada-Bonnefoi C, Laporte D (2004) Kinetics of bubble nucleation in a rhyolitic melt: An
746 experimental study of the effect of ascent rate. Earth Planet. Sci. Lett. 218: 521-537.
747

748 Müller D, Hess KU, Kueppers U, Dingwell DB (2020) Effects of the dissolution of thermal barrier
749 coating materials on the viscosity of remelted volcanic ash. American Mineralogist 105, 1104–1107.
750 Doi: 10.2138/am-2020-7334 1104
751
752 Oswalt JS, Nichols W, O'Hara JF (1996) Meteorological observations of the 1991 Mount Pinatubo
753 eruption, in Fire and Mud: Eruptions and Lahars of Mount Pinatubo, Philippines, edited by Newhall
754 CG and Punongbayan RS, pp. 625– 636, Univ. of Wash. Press, Seattle.
755
756 Pearson D, Brooker R (2020) The accumulation of molten volcanic ash in jet engines; simulating the
757 role of magma composition, ash particle size and thermal barrier coatings. Journal of Volcanology
758 and Geothermal Research 389, 106707
759
760
761 Pierson TC, Major JJ, Amigo A, Moreno H (2013) Acute sedimentation response to rainfall following
762 the explosive phase of the 2008–2009 eruption of Chaitén volcano, Chile. Bull Volcanol. 75:723.
763 Doi: 10.1007/s00445-013-0723-4
764
765 Prata A, Rose WI (2015) Volcanic ash hazards to aviation. The Encyclopedia of Volcanoes, 2nd
766 edition, 911-934.
767
768 Przedpelski ZJ, Casadevall TJ (1991) Impact of volcanic ash from Redoubt Volcano on GE CF6-
769 80C2 turbofan engines. U.S. Geol. Surv. Circ., 1065:36-3
770
771 Rose WI, Delene DJ, Schneider DJ, Bluth GJS, Krueger AJ, Sprod I, McKee C, Davies HL, Ernst
772 GGJ (1995) Ice in the 1994 Rabaul eruption cloud: implications for volcano hazard and atmospheric
773 effects. Nature, 375(6531), 477–479
774
775 Rossi E, Bonadonna C, Degruyter W (2019) A new strategy for the estimation of plume height from
776 clast dispersal in various atmospheric and eruptive conditions. Earth and Planetary Sciences
777 Letters 505:1-12. Doi:10.1016/j.epsl.2018.10.007
778
779 Salinas LJ (2004) Volcanic Ash Clouds Pose a Real Threat to Aircraft Safety. Proceedings of the 2nd
780 International Conference on Volcanic Ash and Aviation Safety. Washington, DC. Session1, p.11-14
781

782 Seligman AN, Bindeman IN, Watkins JM, Ross AM (2016) Water in volcanic glass: From volcanic
783 degassing to secondary hydration. Geochimica et Cosmochimica Acta, 191, 216–238. Doi:
784 10.1016/j.gca.2016.07.010
785
786 Sigmundsson F, Hreinsdóttir S, Hooper A, Árnadóttir T, Pedersen R, Roberts MJ, Óskarsson N,
787 Auriac A, Decriem J, Einarsson P, Geirsson H, Hensch M, Ófeigsson BG, Sturkell E, Sveinbjörnsson
788 H, Feigl KL (2011) Intrusion triggering of the 2010 Eyjafjallajökull explosive eruption. Nature 468,
789 7322, 426-430. Doi:10.1038/nature09558
790
791 Song W, Lavallée Y, Hess KU, Kueppers U, Cimarelli C, Dingwell DB (2016) Volcanic ash melting
792 under conditions relevant to ash turbine interactions. Nature Communications 7:10795. Doi:
793 10.1038/ncomms10795
794
795 Song W, Lavallée Y, Wadsworth FB, Hess KU, Dingwell DB (2017) Wetting and spreading of molten
796 volcanic ash in jet engines. The Journal of Physical Chemistry Letters, 8, 1878–1884.
797
798 Stachowiak GW (2000) Particle angularity and its relationship to abrasive and erosive wear. Wear
799 241, 214–219.
800
801 Sudradjat A, Tilling R (1984) Volcanic hazards in Indonesia: The 1982–83 eruption of Galunggung:
802 Episodes 7, 13–19.
803
804 Tupper A, Oswalt JS, Rosenfeld D (2005) Satellite and radar analysis of the volcanic-cumulonimbi
805 at Mount Pinatubo, Philippines, 1991. J. Geophys. Res., **110,** D09204. Doi:10.1029/
806 2004JD005499.
807
808 Tupper A, Itikarai I, Richards MS, Prata F, Carn S, Rosenfeld D (2007a) Facing the challenges of the
809 international airways volcano watch the 2004/05 eruptions of Manam, Papua New Guinea. Weather
810 Forecast 22(1):175–191
811
812 Tupper A, Guffanti M, Rose B, Patia H, Richards M, Carn S (2007b) The “Gulfstream incident”;
813 Twin-engined flame-out over the Papua New Guinea highlands. In: 4th international work-shop on
814 volcanic ash, Rotorua, New Zealand, 26–30 Mar 2007 [Proceedings]: World Meteorological
815 Organization, Commission for Aeronautical Meteorology, 6 pp

Wadge G, Voight B, Sparks RSJ, Cole PD, Loughlin SC, Robertson RE (2014) An overview of the eruption of Soufrière Hills Volcano, Montserrat from 2000 to 2010. Geol. Soc. Lond. Mem. 39, 1–40. Doi: 10.1144/M39.1

Watanabe K, Ono K, Sakaguchi K, Takada A, Hoshizumi H (1999) Co-ignimbrite ash-fall deposits of the 1991 eruptions of Fugen-dake, Unzen Volcano, Japan. Journal of Volcanology and Geothermal Research 89, 95–112.

Williams ER, McNutt SR (2004) Total water contents in volcanic eruption clouds and implications for electrification and lightning. Proceedings of the 2nd International Conference on Volcanic Ash and Aviation Safety, 67-71

Wilson L, Sparks RSJ, Huang TC, Watkings ND (1978) The control of volcanic column heights by eruption energetic and dynamics. J Geophys Res. 83, 1829–1836

Yamamoto T, Takarada S, Suto S (1993) Pyroclastic flows from the 1991 eruption of Unzen volcano, Japan. Bull Volcanol. 55:166-175

Young S, Sparks S, Robertson R, Lynch L, Aspinall, W (1997) Eruption of Soufriere Hills Volcano in Montserrat Continues. EOS. 78, 38, September, 23, 401-416

Zimanowski B, Wohletz K, Dellino P, Büttner R (2003) The volcanic ash problem. J. Volcanol. Geotherm. Res. 122, 1–5.

Figure Caption

Fig.1. Statistical distribution of damage due to volcanic ash-aircraft encounters as a function of volcanic eruption types. Three types of damage are distinguished. Strombolian-Subplinian eruptions are shown together on this diagram. This is because in basaltic eruptions, too, the eruption cloud can sometimes reach heights of several kilometers. It is also worth mentioning that an eruption can cause different damage simultaneously, such as abrasion and engine problems, which are shown as separate damage.

Fig.2. Results of the statistical analysis applied to the database. The probability of engine failure increases in wet conditions. The Strombolian-Subplinian class eruption in the bottom left corner with the wet line is due to the rainfall condition during the strombolian-type eruption of Pacaya-Guatemela in 1989. The wet graphic line, which also appears in the Pelean eruptions, is due to the heavy rain conditions of the Soufriere Hills and Unzen eruptions. After Eruption-type 4, wet conditions were already in place due to external water.

Fig.3. Starting material (Nescher, PDC, France). ABCD: SEM pictures, EFGH: Minerals under a binocular microscope, I: Whole rock chemical analysis

Fig.4. SEM photomicrographs showing overviews of the A and B from the NAsh-AnH1 and 2 samples and C and D from the NAsh-H sample. Rugged, globular, bulbous texture is observed in both states (Anhydrous and Hydrous). In the NAsh-H sample, ellipsoidal formations are more common.

Fig.5. SEM photomicrograph of the surface of the hydrous sample at high magnification. The small euhedral crystals rest on a glassy material in which they are more or less immersed,

indicating incipient melting of the volcanic ash. Corresponding chemical analysis gives mineraloid+crystal analysis values rather than a mineral analysis. Partly Alkali feldspar and partly glass chemistry coexist. In this case, it can be accepted as a result of melting. Note the abundance of acicular crystals.

Fig.6. Fig6.A. FIB-SEM image of NAsh-AnH. The presence of mineraloid droplets at the base is observed. Spectrum points correspond to the chemical analyses given in the SI. The newly formed crystallites are also generally associated with prismatic minerals.
6.B. An intact piece of pumice with slight melting from the edges is observed in the NAsh-AnH. The melting zone is observed as a brighter-whitish band.
6.C. The spherical droplet of mineraloid in NAsh-H and the same invading mineraloid with numerous secondary crystallites.
6.D. Pumice fragments in NAsh-H have widely melted and started to disappear.

Fig.7. SEM-FIB laser engraving, we see acicular feldspars forming vaguely below the surface as phantom minerals in mineral gel (in hydrous sample). Step-like melting is obvious in the hydrous sample interior.

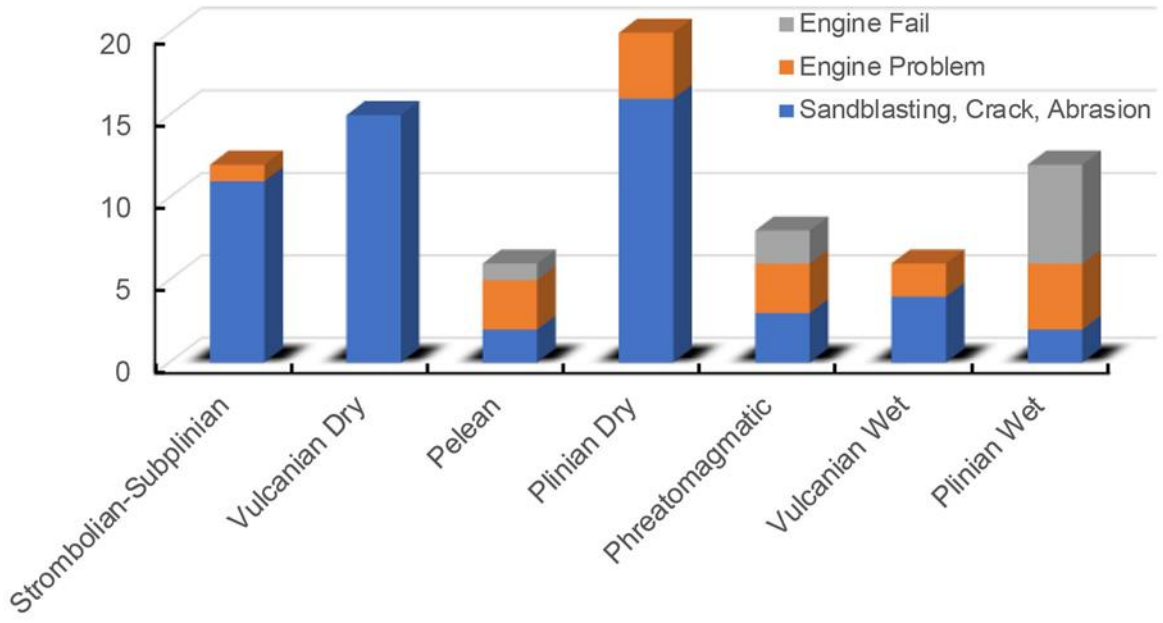
20
15
10
5
0
Engine Fail
Engine Problem
Sandblasting, Crack, Abrasion
Strombolian-Subplinian
Vulcanian Dry
Pelean
Plinian Dry
Phreatomagmatic
Vulcanian Wet
Plinian Wet

892

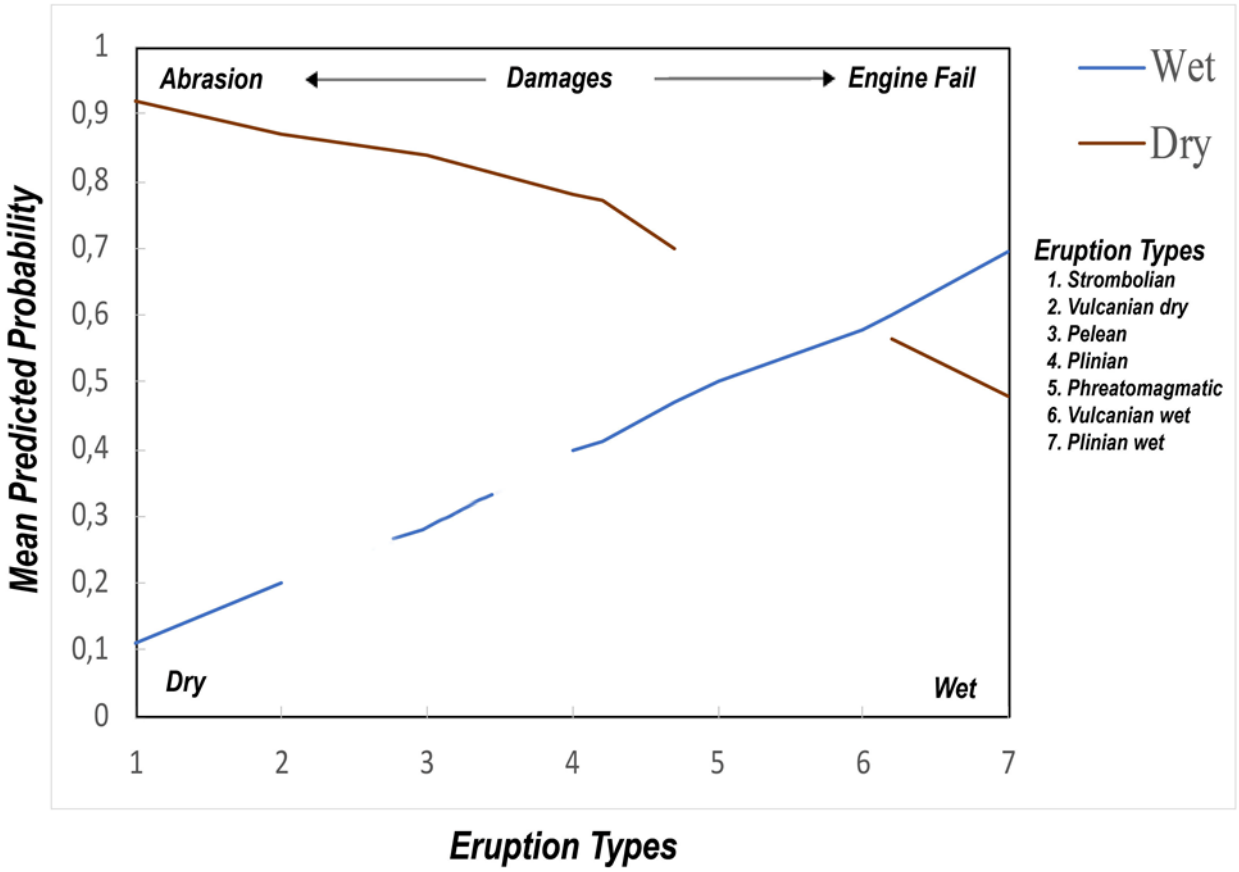
Mean Predicted Probability
1
0,9
0,8
0,7
0,6
0,5
0,4
0,3
0,2
0,1
0
Abrasion
Damages
Engine Fail
Dry
Wet
1
2
3
4
5
6
7
Eruption Types
Wet
Dry
Eruption Types
1. Strombolian
2. Vulcanian dry
3. Pelean
4. Plinian
5. Phreatomagmatic
6. Vulcanian wet
7. Plinian wet

893

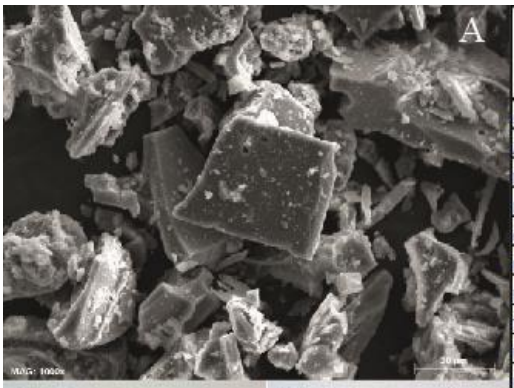

I

Sample	Neschers
SiO2 %	60,55
Al2O3 %	17,95
Fe2O3 %	3,19
MgO %	0,80
CaO %	2,02
Na2O %	4,91
K2O %	5,50
TiO2 %	0,75
MnO %	0,15
P2O5 %	0,15
Ba %	0,06
Sr %	0,02
H2O+ %	0,80
H2O- %	2,82
Total %	99,67

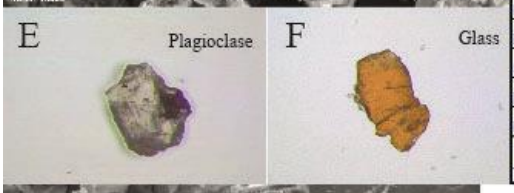

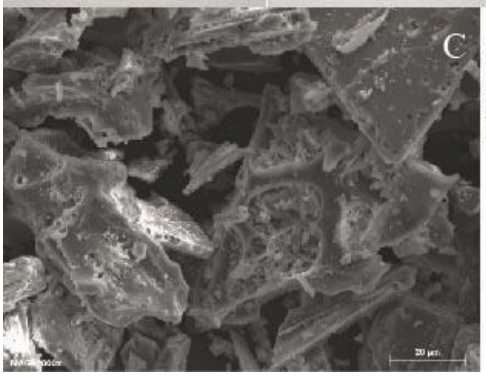

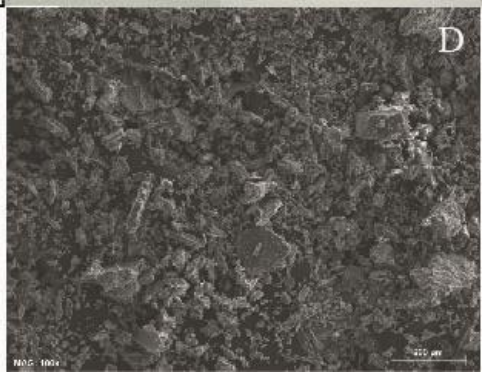

Fig . Starting material (Nescher PDC)
A.B.C.D.: SEM pictures
E.F.G.H.: Minerals under binocular microscope
I: Whole rock chemical analysis

894

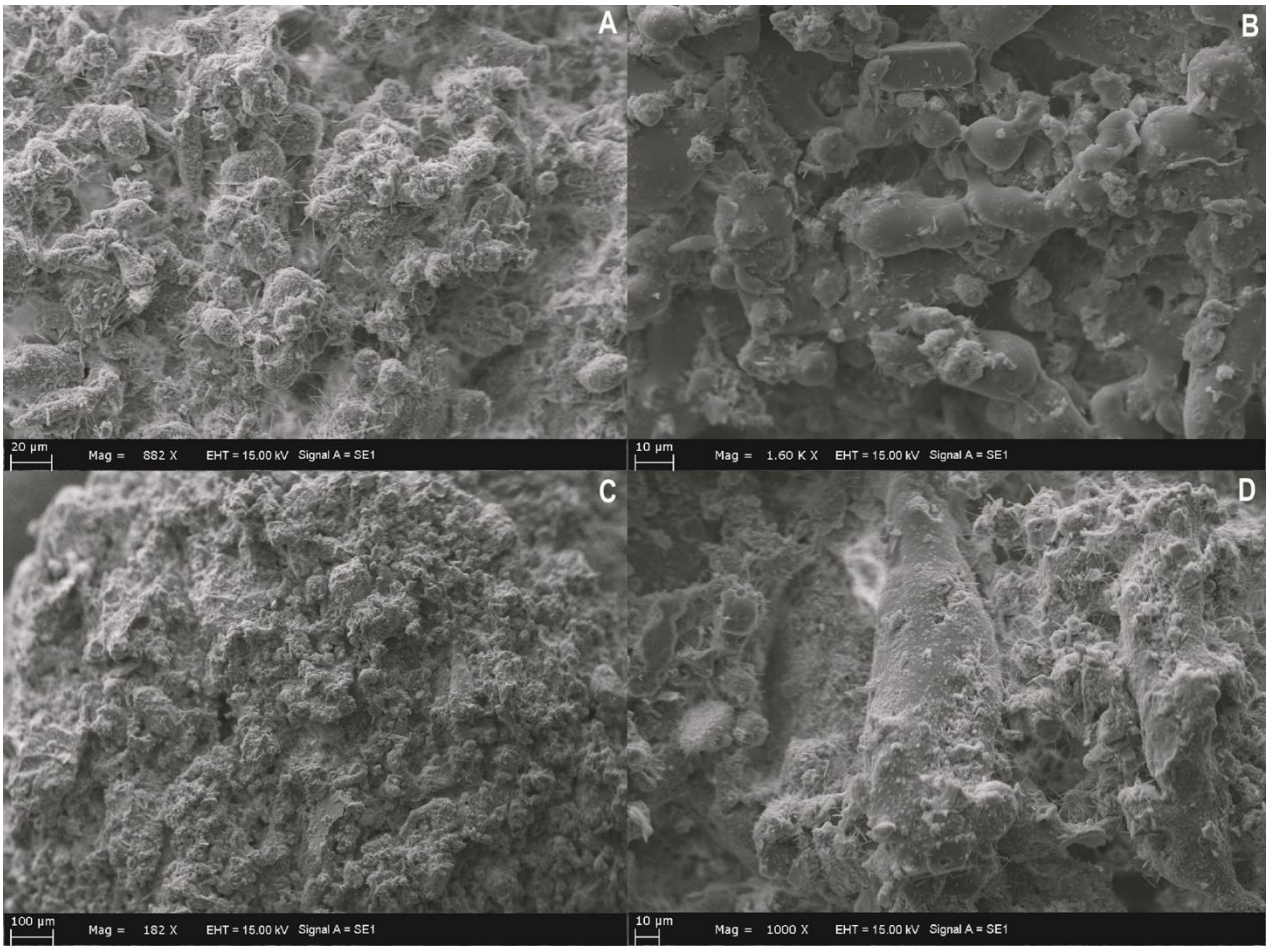
A
20 µm
Mag = 882 X
EHT = 15.00 kV
Signal A = SE1
B
10 µm
Mag = 1.60 K X
EHT = 15.00 kV
Signal A = SE1
C
100 µm
Mag = 182 X
EHT = 15.00 kV
Signal A = SE1
D
10 µm
Mag = 1000 X
EHT = 15.00 kV
Signal A = SE1

895

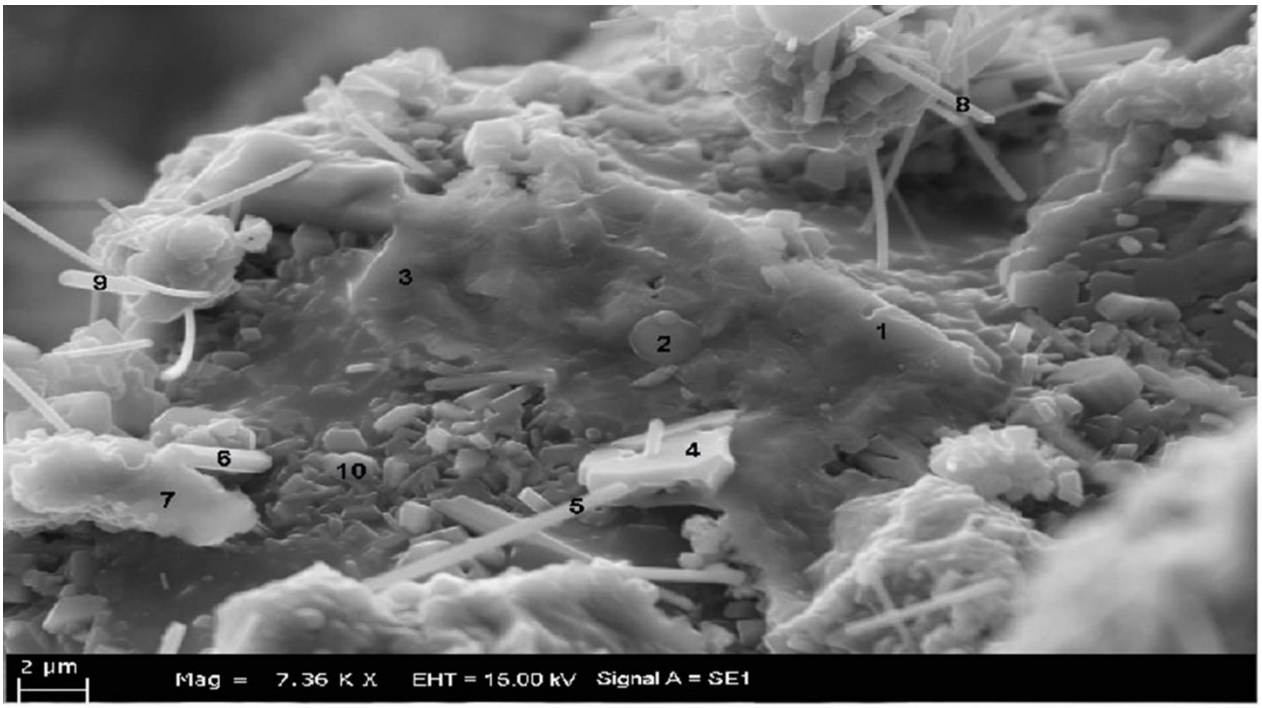

	1	2	3	4	5	6	7	8	9	10
Na2O	3,18	4,00	3,01	4,77	4,06	3,85	4,51	2,64	4,50	4,14
MgO	0,77	1,32	0,04	0,88	1,30	0,38	0,74	0,92	0,76	0,08
Al2O3	16,47	18,96	16,94	19,00	16,71	16,67	20,09	16,55	19,80	17,85
SiO2	60,83	58,13	62,48	66,46	61,35	60,85	60,14	63,29	58,30	65,58
K2O	9,03	6,88	8,65	6,49	7,05	7,30	6,39	8,03	7,26	6,71
CaO	2,89	3,20	1,73	0,94	2,01	1,81	1,14	2,01	1,51	1,40
TiO2	1,44	0,73	0,14	0,00	1,01	1,08	0,39	1,12	0,37	0,39
MnO	0,30	0,38	0,28	0,00	0,11	0,00	0,00	0,53	0,14	0,49
FeO	3,45	2,48	2,42	2,68	4,38	3,09	2,77	3,23	2,86	2,49
Total	98,35	96,09	95,70	101,24	97,98	95,02	96,16	98,32	95,50	99,12

896

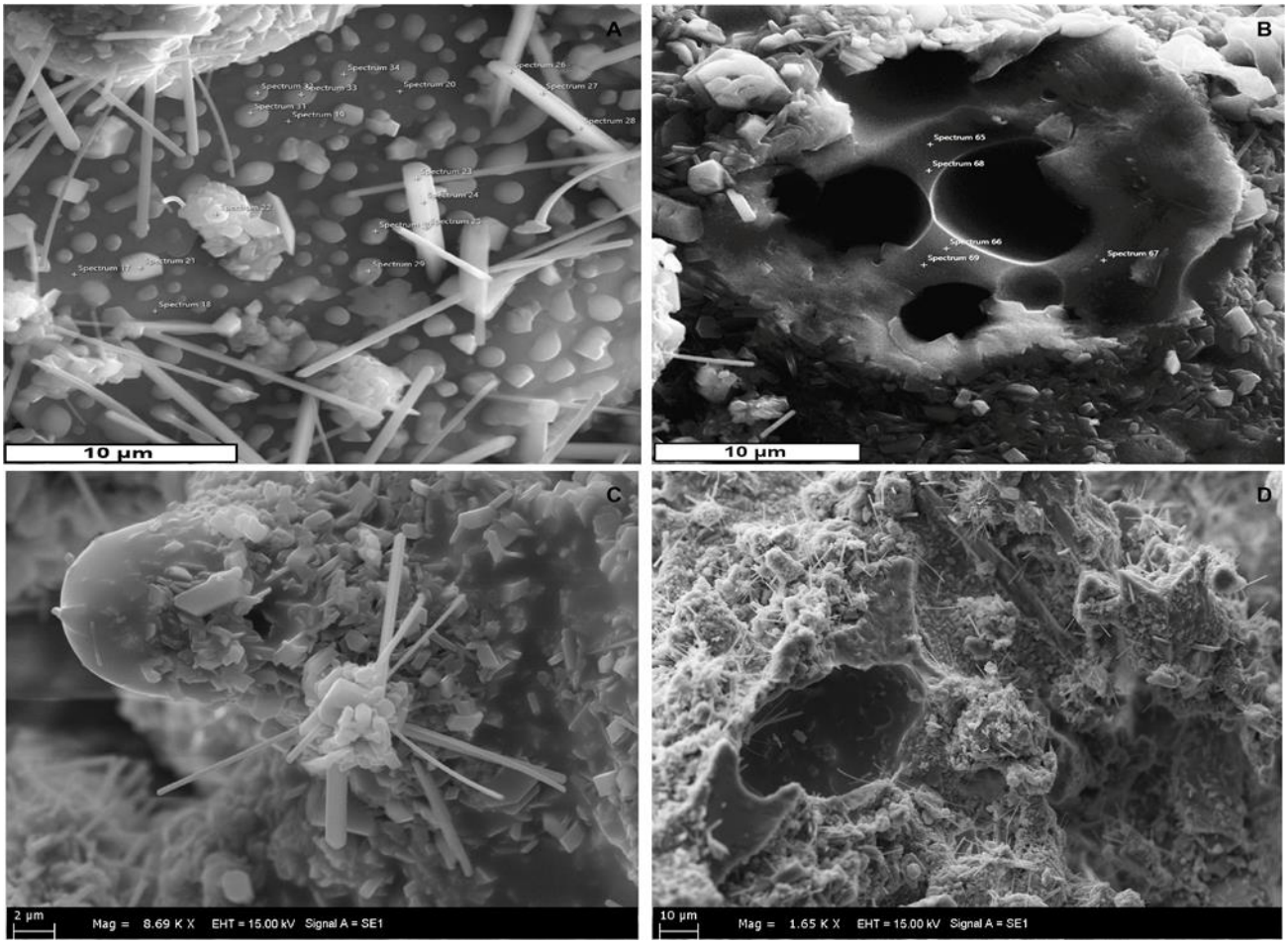
A
Spectrum 34
Spectrum 26
Spectrum 32
Spectrum 33
Spectrum 20
Spectrum 27
Spectrum 31
Spectrum 19
Spectrum 28
Spectrum 23
Spectrum 24
Spectrum 22
Spectrum 25
Spectrum 21
Spectrum 17
Spectrum 29
Spectrum 18
10 µm
B
Spectrum 65
Spectrum 68
Spectrum 66
Spectrum 69
Spectrum 67
10 µm
C
2 µm
Mag = 8.69 K X EHT = 15.00 kV Signal A = SE1
D
10 µm
Mag = 1.65 K X EHT = 15.00 kV Signal A = SE1

897

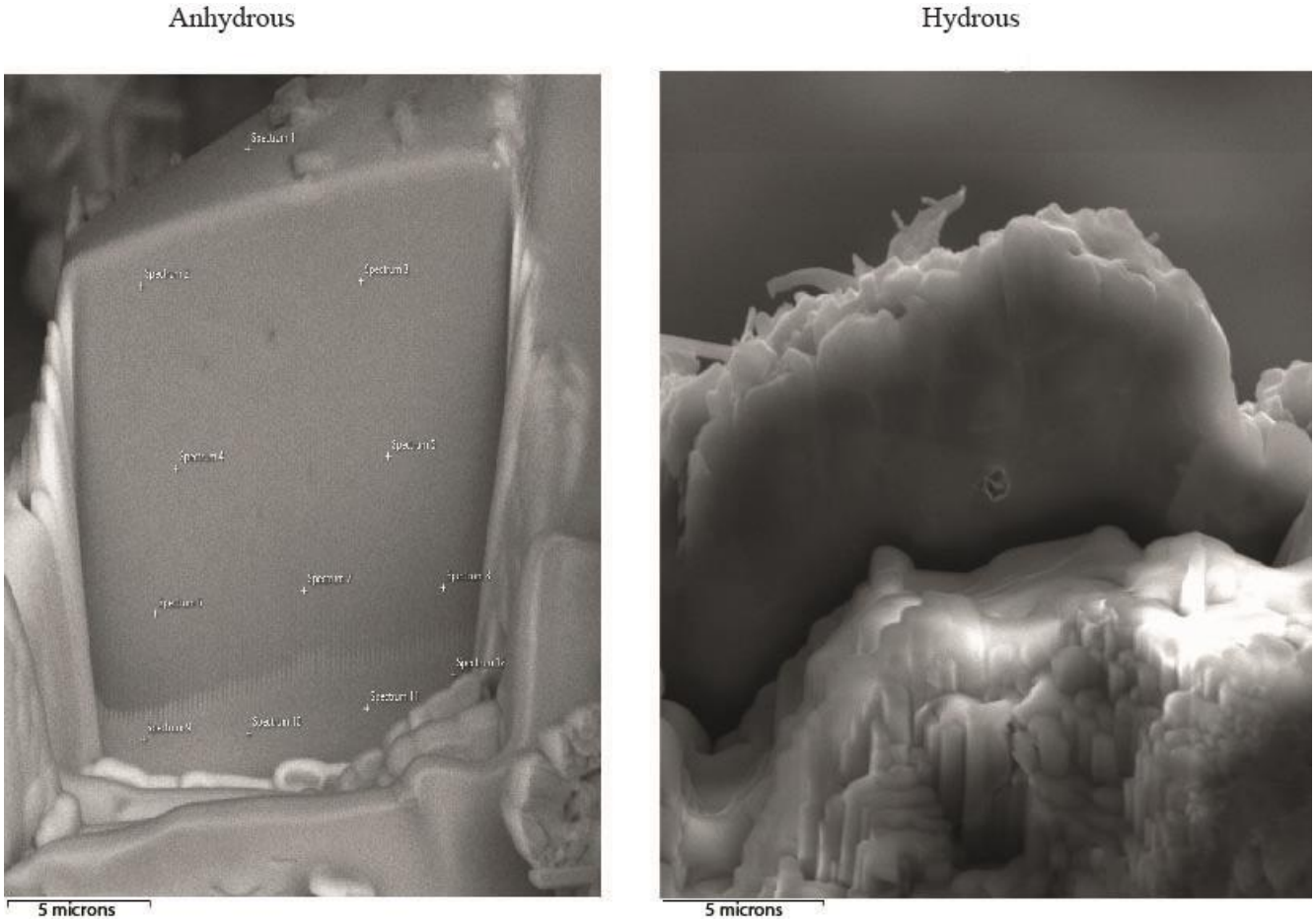

Supplementary Information

Supplementary Figures

SI-Fig1. SEM images of the starting material, which is very rich in pumice fragments, glass shards and minerals. There are no secondary melting traces.

SI-Fig2. Anhydrous samples after melting experiments. Botryoidal texture is dominant, but pumices and minerals are mainly conserved. Secondary mineral growths are present.

SI-Fig3. SEM images of Hydrous sample after melting experiments. Pumices, glass shards and minerals show the melting textures, and the basement represents the mineraloid melt with intensive secondary mineralisations.

Supplementary Tables

911 **SI-Table1.** Compilation of aircraft encounters with volcanic ash clouds, 1953–2009, as a Microsoft
912 Excel 93–2007 spreadsheet file (.xls) (modified from Guffanti et al., 2010, the columns in red have
913 been added).
914 **SI-Table2.** Statistical distribution of the damage
915